

Traffic Response Functions: Patterns, Propagation and Congestion

Sebastian Gartzke*, Shanshan Wang, Thomas Guhr and Michael Schreckenberg

Faculty of Physics, University Duisburg–Essen, Lotharstraße 1, 47048 Duisburg, Germany

June 5, 2024

Abstract

Using empirical data gathered on motorways in Germany, we follow a new approach by further exploring response functions as a possible tool to study traffic dynamics in motorway networks. We uncover the basic characteristics of responses of flow and density to given signals and the capability of responses to capture the correlation between these fundamental observables. Furthermore, we uncover the potential use of responses to characterize traffic patterns. We are able to demonstrate the differentiation of congestion patterns and the determination of the propagation velocity of moving congestion.

Keywords: response functions, traffic congestion, vehicular traffic, time series analysis, complex system

Contents

1	Introduction	2
2	Data description and methods	2
2.1	Data	2
2.2	Response functions and congestion indicators	3
3	Studied locations	5
4	Results	8
4.1	A comparison of responses of velocity, flow and density	8
4.2	On- and off-ramp propagation of congestion and generic response features	10
4.3	Differences in congestion patterns	12
4.4	The propagation velocity of congestion	15
4.5	Scaling of responses	16
5	Conclusion	16
	References	21
	Appendices	22
	Appendix A	22
A.1	Interchange Breitscheid: supplementary map	22
A.2	Different representation of responses	23

*sebastian.gartzke@uni-due.de

1 Introduction

Vehicular traffic on a multi-lane motorway is a highly complex and dynamic process. Nevertheless, millions of traffic participants experience this complexity on daily basis due to a rather simple fact that seems to be inevitable, namely the fact of traffic congestion. Although it may seem very simple to the individual driver, congestion is a phenomenon emerging in a collective driven many-body system which unfolds its complex dynamics in different scales of space and time. Over the last six decades a large variety of theories and models has been developed to understand and describe the complex, non-linear behavior of traffic systems, e.g. [1–15] and others. Due to the fact that vehicular traffic is a key element of modern society’s mobility and transportation it is a desirable task to continuously study traffic networks. The development of alternative research approaches and methods helps to understand these systems and their dynamics much better and find new tools for effective traffic planning, management and control.

Recently, we successfully conducted several studies along these lines [16–20], focusing on the application of concepts and approaches for studying financial markets on traffic networks. By extensively studying traffic data with correlation matrices, we identified dominant and subdominant collectivities in traffic, revealing new characteristics of traffic networks. The most recent work in [20] uncovers the potential application of response functions as a tool for studying traffic dynamics. The basic idea behind the concept of response functions is being able to study a systems reaction to specific events, revealing their influence on and the sensitivity of the response variable. The applications of response functions in financial markets have successfully revealed the influence of different time scales on non-Markovian effects [21–26]. In case of vehicular traffic, congestion on motorways is certainly one of the most interesting and significant events to which responses of traffic observables can be studied. By choosing the velocity as a response variable, response functions are able to capture the presence of congestion, its propagation along motorway segments and therefore spatiotemporal features of present traffic patterns [20]. These findings lay an important foundation for the study of traffic networks with the concept of response functions. However, the attempt of fully characterizing traffic patterns is a difficult but crucial task and information on other fundamental observables, such as density and flow, are desirable.

With this contribution we aim to deepen the understanding of the possibilities of response functions as a tool for the study of traffic dynamics. For this sake, we extend the previous approach in [20] by also incorporating flow and density responses for spatially subsequent motorway sections. By comparing all three types of responses we aim to uncover the basic characteristics of flow and density responses. Furthermore, we define multiple congestion indicators according to different velocity ranges. The goal is to identify different phases or patterns of congestion. In the course of this we investigate the possibility of deriving the propagation velocity of congestion with the help of responses.

This paper is organized as follows. Sec. 2 presents the studied data set and introduces response functions and associated indicators for congestion. Sec. 3 introduces the locations we use to conduct the study. The results are presented in Sec. 4. Lastly, Sec. 5 briefly summarizes and concludes our results.

2 Data description and methods

For our study we use traffic data gathered by inductive loop detectors on motorways in North Rhine-Westphalia (NRW), Germany. In the following we describe the used data in Sec. 2.1 and present the methods conducted in our study in Sec. 2.2.

2.1 Data

Inductive loop detectors on motorways gather information about the traffic situation by recording essential observables on each lane, such as traffic flow rate q and average velocity v [27]. At each section the measurements are conducted over time intervals of one minute and the aggregated data are given in units of vehicles/h and km/h, respectively. In addition, the detectors distinguish cars and trucks. Our study focuses on workdays, therefore we exclude weekends and public holidays, leaving

a total number of $N = 243$ workdays from our data set recorded from December 2016 to December 2017.

For the purpose of this study we combine the data of all lanes at each section into one effective lane as follows. For each lane l at each section s we determine a traffic density

$$\rho_{sl}^{(m)}(t) = \frac{q_{sl}^{(m)}(t)}{v_{sl}^{(m)}(t)}, \quad (1)$$

with $m = \text{car, tr}$, for cars and trucks separately. The sum of the respective quantities of cars and trucks yield the total traffic flow and density

$$q_{sl}(t) = q_{sl}^{(\text{car})}(t) + q_{sl}^{(\text{tr})}(t), \quad (2)$$

$$\rho_{sl}(t) = \rho_{sl}^{(\text{car})}(t) + \rho_{sl}^{(\text{tr})}(t), \quad (3)$$

for each lane. The total, effective flow $q_s(t)$ and density $\rho_s(t)$ for each section result from the summation over all lanes. Finally, the corresponding effective velocity $v_s(t)$ at each section is given by

$$v_s(t) = \frac{q_s(t)}{\rho_s(t)} = \frac{\sum_l q_{sl}(t)}{\sum_l \rho_{sl}(t)}. \quad (4)$$

Even though using the hydrodynamic relation in Eq. (1) is a common procedure for the determination of traffic densities from loop detector data, we like to point out, for the sake of completion, that it has to be considered as an approximation. Here we determine a spatial quantity from a temporal quantity, which can result in systematic errors [27]. By using the time mean speed for calculation with Eq. (1), instead of the spatial mean speed, the true density is usually underestimated. However, in most cases the approximation is considered sufficient because the main characteristics of macroscopic traffic effects are preserved.

2.2 Response functions and congestion indicators

This contribution focuses on the analysis of response functions

$$\tilde{R}_{ij}^{(x)}(\tau) = \frac{\sum_{t=1}^{T-\tau} (x_i(t+\tau) - x_i(t)) \varepsilon_j(t)}{\sum_{t=1}^{T-\tau} \varepsilon_j(t)} = \frac{\langle \Delta x_i(t, \tau) \varepsilon_j(t) \rangle_t}{\langle \varepsilon_j(t) \rangle_t}, \quad (5)$$

where $\tilde{R}_{ij}^{(x)}(\tau)$ yields the response, i.e. the average change, of a traffic observable x at section i at time $t + \tau$ conditioned on congestion indicated by $\varepsilon_j(t)$ at section j at a previous time t . With regard to [20], we take a first step to extend the study by not only considering the responses of velocities $x = v$, but also determining and discussing the responses of flow $x = q$ and density $x = \rho$. In a second step, we take into account the complex nature of freeway traffic by varying the indicator $\varepsilon_j(t)$. Alternatively one could also define response functions in which the unconnected part $\langle \Delta x_i(t, \tau) \rangle_t \langle \varepsilon_j(t) \rangle_t$ is subtracted. Here we find it useful to use the definition in Eq. (5).

On the one hand, in a relatively simple approach congestion can be described as a (density) shock wave propagating up-stream through free flow traffic phases [1, 3]. On the other hand, more recent traffic theory approaches show the existence of different phases (or states) of congestion and their transitions, whose description is far more complicated, e.g. three-phase traffic theory [14, 15]. In light of the research in [20], we have an idea of the properties that response functions may capture in relation to congestion phases. We expect to find the capability of responses to reflect the correlations between the fundamental traffic observables velocity, flow and density during phases of congestion propagation as depicted in Fig. 1. We try to deepen the study on traffic dynamics by using response functions with

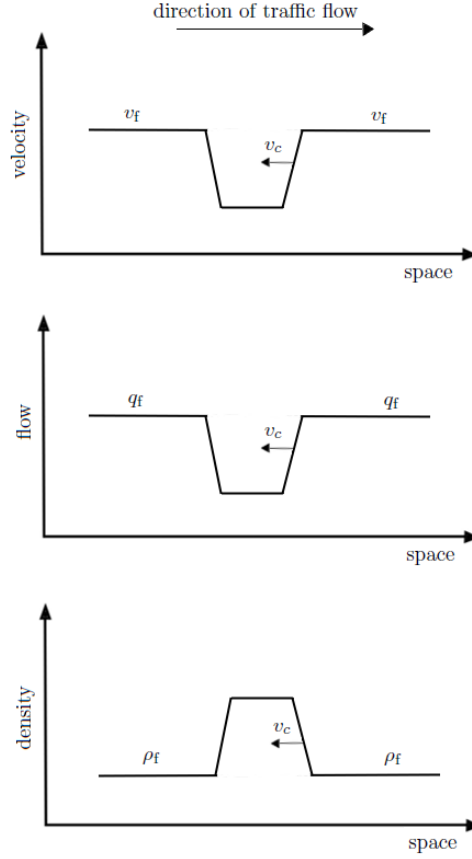


Figure 1: Schematic representation of congestion propagation against the direction of free traffic flow with velocity v_c at a fixed time t . The homogeneous distribution of velocity v_f , flow q_f and density ρ_f during a free flow phase is perturbed by a (density) shock wave. The sketch was drawn with Paint.net [30].

four different indicator functions

$$\begin{aligned} \varepsilon_j^{(0)}(t) &= \begin{cases} 1, & \text{if } 0 \leq v_j(t) \leq 20 \text{ km/h,} \\ 0, & \text{else,} \end{cases} & \varepsilon_j^{(1)}(t) &= \begin{cases} 1, & \text{if } 20 \text{ km/h} < v_j(t) \leq 40 \text{ km/h,} \\ 0, & \text{else,} \end{cases} \\ \varepsilon_j^{(2)}(t) &= \begin{cases} 1, & \text{if } 40 \text{ km/h} < v_j(t) \leq 60 \text{ km/h,} \\ 0, & \text{else,} \end{cases} & \varepsilon_j^{(3)}(t) &= \begin{cases} 1, & \text{if } 0 \leq v_j(t) \leq 60 \text{ km/h,} \\ 0, & \text{else.} \end{cases} \end{aligned} \quad (6)$$

More than one indicator function help to capture different phases of congestion occurrence such as stop-and-go traffic, wide moving jams, and others. In this way, we also show an example for the flexible applications of response functions according to different research purposes. While $\varepsilon^{(0)}(t)$ indicates heavily congested sections with low velocity range in Eq. (6), $\varepsilon^{(1)}(t)$ and $\varepsilon^{(2)}(t)$ aim to indicate situations like stop-and-go traffic or phases between two congestion waves. Incorporating the velocity ranges of the previous indicators, $\varepsilon^{(3)}(t)$ represents a more generous threshold for the indication of congestion. It is mainly introduced for the sake of comparison.

Our work focuses on rush hours to study the traffic responses to congestion, more specific on either morning rush hours (mr) from 06:00 to 11:00 or afternoon rush hours (ar) from 14:00 to 19:00, depending on the individual cases to be examined. The time lag in Eq. (5) is restricted to $\tau = 300$ min covering the whole time interval of the rush hours. To avoid capturing responses to random events, e.g. accidents or daily construction sites, in this study response functions are averaged over the given work days. We generally proceed as follows: For each case examined, we start by choosing an indicator section j and convert all given time series of velocities $v_j(t)$ into four times series of indicators $\varepsilon_j^{(y)}(t)$, $y = 0, 1, 2, 3$ according to Eq. (6). For each day and each pair of sections ij the corresponding response functions $\tilde{R}_{ij}^{(x)}(\tau)$ are calculated for all three observables velocity, flow and density from section i for all

four types of indicators from section j . Averaging the calculated responses over all given days results in the averaged response function $R_{ij}^{(x)}(\tau)$, $x = v, q, \rho$, respectively, for each given indicator.

3 Studied locations

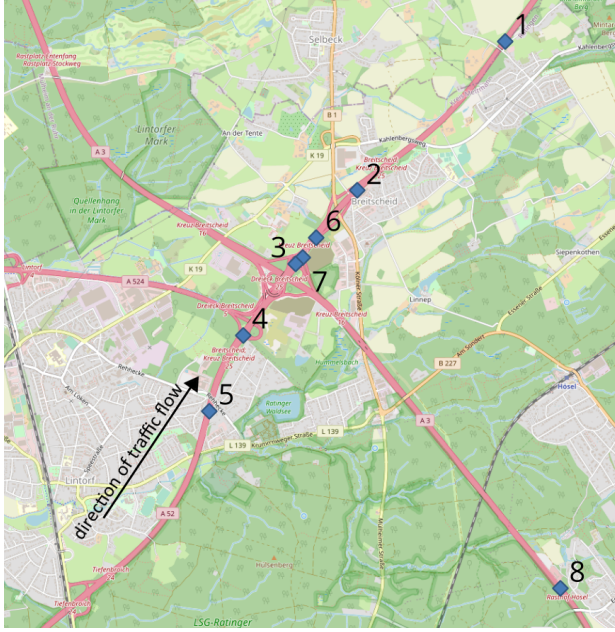
Motorway interchanges are important junctions in traffic networks and usually provide more than one function. They establish a connection between two (or more) motorways, they allow traffic participants to change the course of direction and, in some cases, they function as an entry point into the motorway network. Unfortunately, as useful as they are, interchanges also have downsides during heavily trafficked periods. Due to their structure, combined with the fact that on- and off-ramps act as bottlenecks [14, 15], motorway interchanges are very likely to be an origin of traffic congestion during rush hours. This is especially the case for motorway interchanges connecting regularly high trafficked motorways. Apart from inducing traffic congestion, motorway interchanges are capable of spreading congestion into other parts of the motorway network they connect with. As a result, congestion may propagate through on- and off-ramps onto connected motorways or urban traffic networks, which subsequently leads to a deterioration of the present traffic situation.

With regard to the characteristics mentioned above, we consider motorway interchanges and connected motorways for our study. We explore three different, heavily trafficked motorway segments in NRW, Germany. Two of these segments are motorway interchanges while the third is a part of motorway A3 connecting two interchanges. All three studied locations including the sections with loop detectors are shown in Fig. 2. The numbering of sections is chosen in a way that the direction of traffic flow goes from larger section numbers to smaller section numbers. As a consequence, congestion propagates from smaller section numbers to larger section numbers. The calculation of responses is done on spatially subsequent sections. In addition, Fig. 3 illustrates the overall traffic situation on workdays with averaged data for all studied locations. Here we would like to take the opportunity to point out that the velocity in Figs. 3 and 4 in [18] are given in the unit of veh/min instead of veh/h.

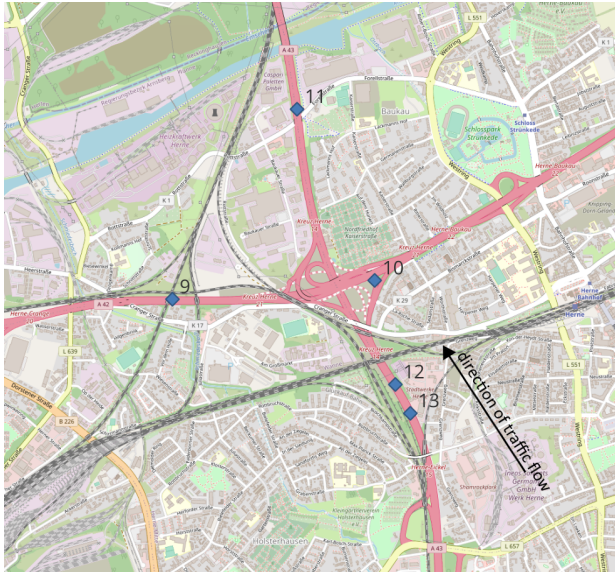
Figure 2(a) shows the motorway interchange Breitscheid, which connects three motorways, namely A52, A3 and A524. Motorway A3 is a longer ranged motorway directly connecting big cities like Cologne (in south direction), Duisburg and Oberhausen (in north direction). Motorway A52 is a shorter ranged motorway which establishes a direct connection between the cities Düsseldorf (in south-west direction) and Essen (in north-east direction). As shown in Fig. 3(a), the segment of A52 in north-east direction, going from Düsseldorf to Essen, is heavily trafficked during rush-hours and congestion is present on daily basis. In addition, the traffic situation is complicated because traffic participants are able to leave and enter the motorway network before passing section 6 and section 2, respectively. Section 6 is a special case due to the general structure of the interchange Breitscheid. It is located on a separated lane which routes the traffic flow from connected motorways, merging it with the traffic on the main lanes of A52 between section 2 and section 1 (see supplementary map in Fig. A1 in Appendix A.1). For the conducted investigations section 1 will be the indicator section.

Motorway interchange Herne, shown in Fig. 2(b), connects motorway A42 and A43. While the former provides a connection of large cities of the Ruhrgebiet (Ruhr area), such as Gelsenkirchen, Bottrop, Oberhausen and Duisburg (from east to west), the latter connects the city of Herne with Wuppertal, Bochum, Recklinghausen and Münster (from south to north). The overall amount of traffic within interchange Herne is not quite as high as in the case of interchange Breitscheid, but Fig. 3(b) clearly demonstrates the occurrence of congestion on regular bases during rush-hours. Depending on the study case, sections 11 and 9 will be the indicator sections for our investigation.

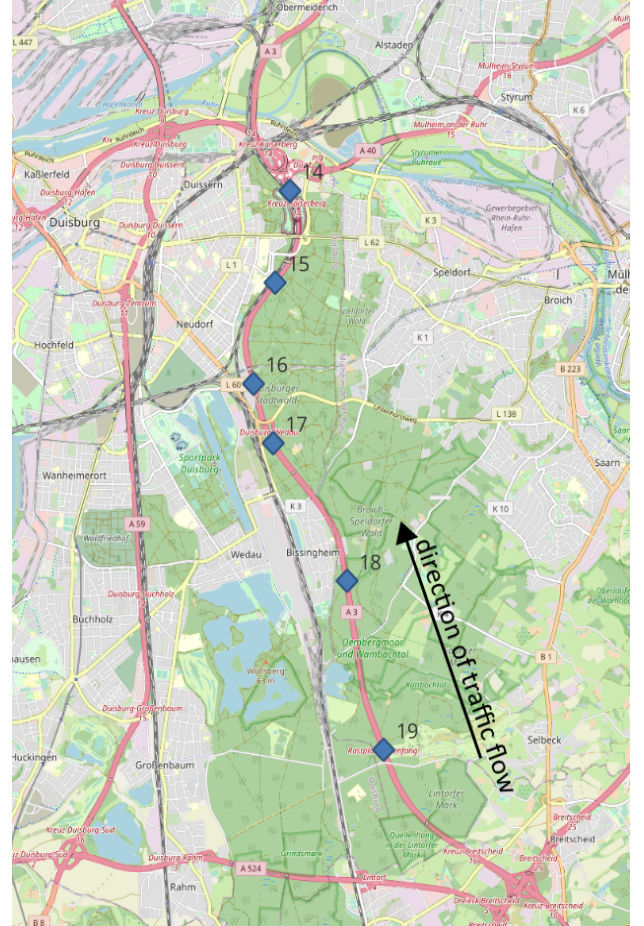
The third location is the segment of motorway A3 between interchanges Breitscheid and Kaiserberg, see Fig. 2(c). This part of the A3 is heavily trafficked in north direction during afternoon rush-hours on daily basis. Within interchange Kaiserberg, near section 14 and (spatially) right next to an off-ramp, the number of main lanes reduces from three to two. This reduction acts as an additional bottleneck, reducing the capacity of the motorway and inducing heavy congestion on regular basis. Figure 3(c) demonstrates how severe the congestion is on average and how far the traffic breakdown propagates into the south. Due to the traffic situation within interchange Kaiserberg, we choose section 14 as the indicator section for our investigation.



(a) Breitscheid



(b) Herne



(c) Motorway A3 between Breitscheid and Kaiserberg

Figure 2: Locations of loop detectors (blue markers) for all three study cases. (a) Motorway interchange Breitscheid, (b) motorway interchange Herne and (c) motorway A3 between interchange Breitscheid and Kaiserberg. The numbering of sections is chosen in such a way that the direction of traffic flow goes from larger section numbers to smaller section numbers. All map data and map tiles are provided by OpenStreetMap ©OpenStreetMap Contributors and are licensed under ODbL v1.0 by the OpenStreetMap Foundation [28, 29].

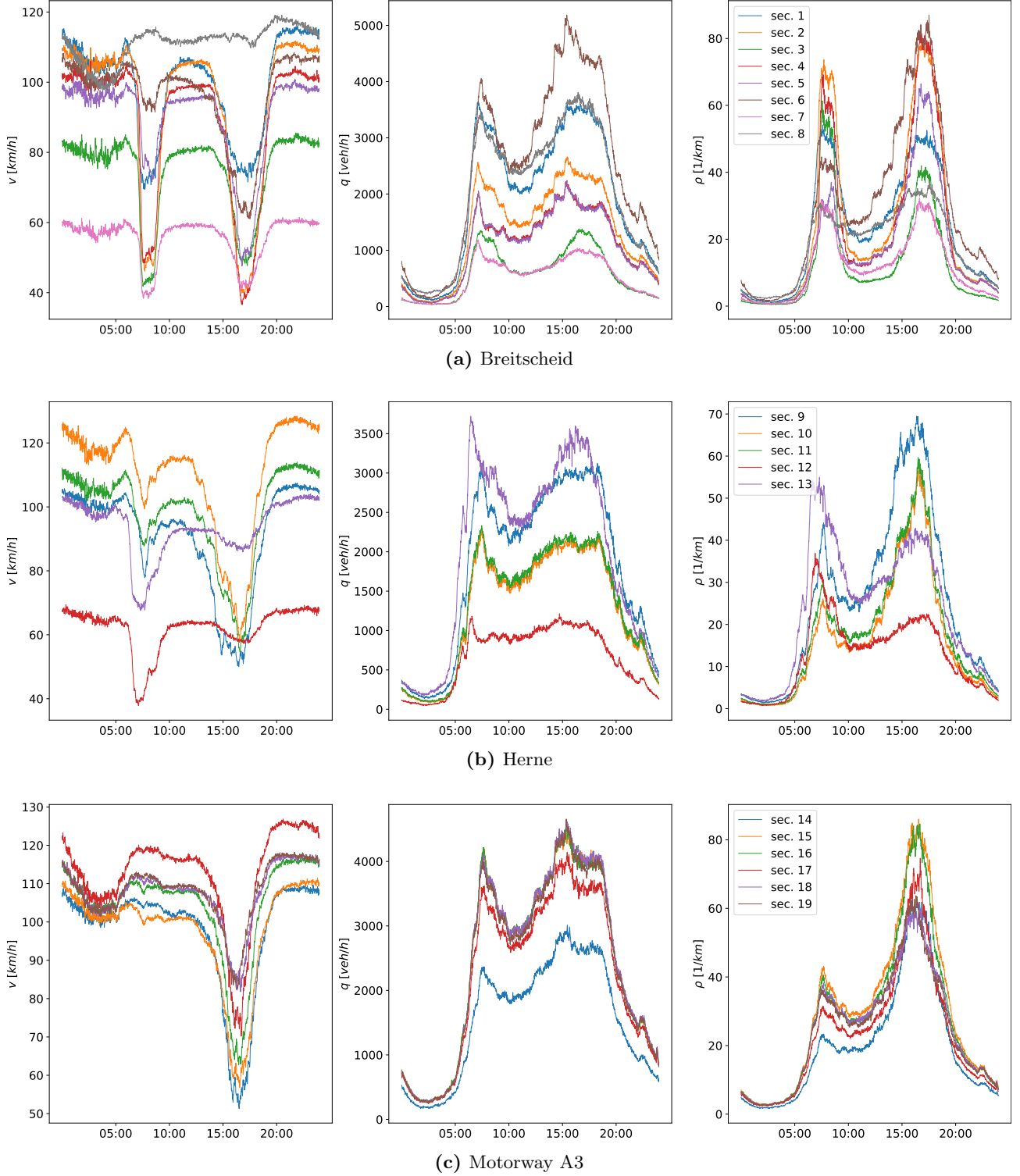


Figure 3: Time evolution of effective flow q , velocity v and density ρ at all sections averaged over all $N = 243$ workdays. The averaged data yields a representation for the usual traffic situation on workdays at the three different motorway segments shown in Fig. 2. Distinct breakdowns in the averaged velocity time-series during the rush hours clearly indicate the occurrence of congestion on regular basis.

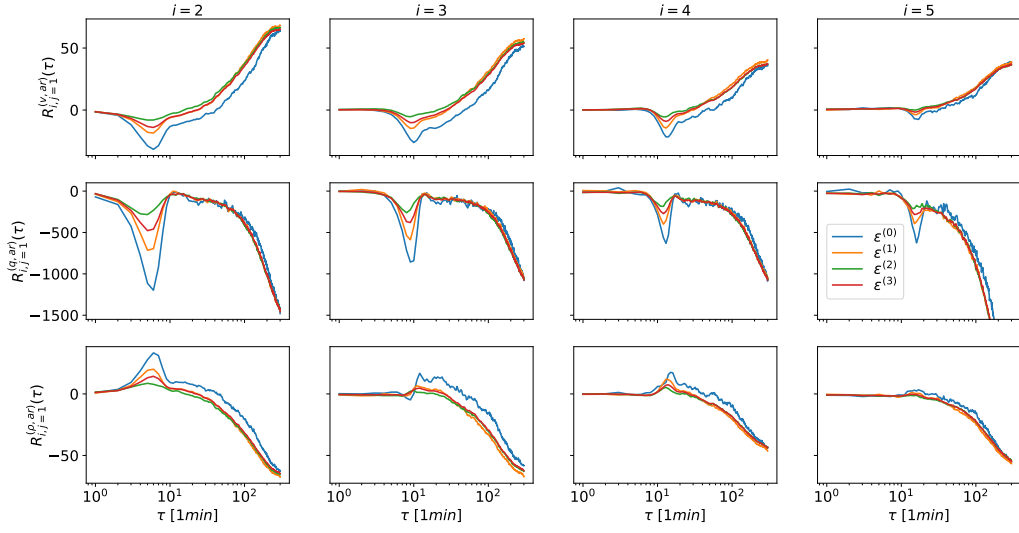
4 Results

4.1 A comparison of responses of velocity, flow and density

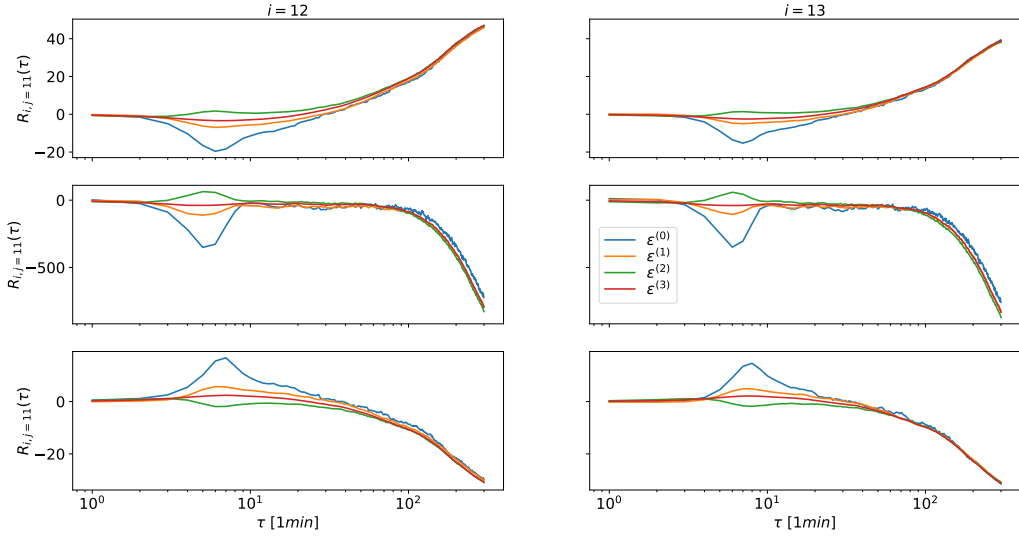
A convenient starting point for our analysis is to briefly relate this study to previous results from [20], in which interchange Breitscheid was already a location of investigation. Figure 4(a) shows velocity, flow and density responses of spatially subsequent sections to congestion at section 1 for all used indicators during afternoon rush hours. Despite a different velocity range of indicator $\varepsilon^{(0)}(t)$ for heavy congestion (up to 20 km/h instead of 10 km/h used in [20]), one can easily identify similar behavior of velocity responses by comparison. The responses of neighboring sections 2 to 5 show negative values, forming dipping-downs or local minima, for smaller time lags and increase to positive values, continuously growing for greater τ . The occurrence of response valleys, as well as their amplitude and width, depend on the distance between indicator section j and the responding section i . With increasing distance the valleys occur at greater time lag with shrinking width and amplitude. This response behavior captures and reflects the velocity breakdown and therefore the upstream propagation of congested traffic. By comparison, we find the behavior of velocity responses for $\varepsilon^{(0)}(t)$ at interchange Breitscheid is the same as the ones at interchange Herne in Fig. 4(b) and on motorway A3 in Fig. 4(c). This demonstrates that the velocity responses for $\varepsilon^{(0)}(t)$ are independent of the studied location.

Before we discuss the response for other indicators, we take a first look at flow and density responses for indicator $\varepsilon^{(0)}(t)$ in Fig. 4. Even though the flow has a very fluctuating nature on shorter time scales (a couple of minutes), the average responses show very clear courses, including sharp local minima which occur at larger time lags with increasing distance to the indicator section. This is the case for all three studied locations in Fig. 4. The amplitudes of the negative responses of the nearest neighboring sections to the indicator section at Breitscheid ($i = 2$) and motorway A3 ($i = 15$) in Fig. 4(a) and (c) corroborate the severity of the occurring congestion at these locations. Values between -1000 veh/h and -1200 veh/h clearly demonstrate the heavy traffic breakdown already indicated by the average data in Fig. 3. A comparison of velocity and flow responses with the density responses in Fig. 4 reveals fulfilled expectations regarding their courses. Due to the fact that traffic breakdowns induce a local increase in density, the respective density responses actually show local maxima which occur at larger time lags τ for increasing distance to the indicator section. Also, in case of density response the scaling of the amplitudes reflect the severeness of the traffic jam at Breitscheid and on A3 in Fig. 4(a) and (c). With values over 20 veh/km for the nearest responding section the local increase in density amounts to a fourth of the average value shown in Fig. 3. Overall, we find that the local minima and maxima of all response types occur at the same time lag τ for the individual responding sections. Therefore, the responses of all three observables for $\varepsilon^{(0)}(t)$ clearly capture the propagation of congestion and the correlations between velocity, flow and density as depicted in Fig. 1. This finding is a fundamental basis for response functions as a tool to study traffic dynamics.

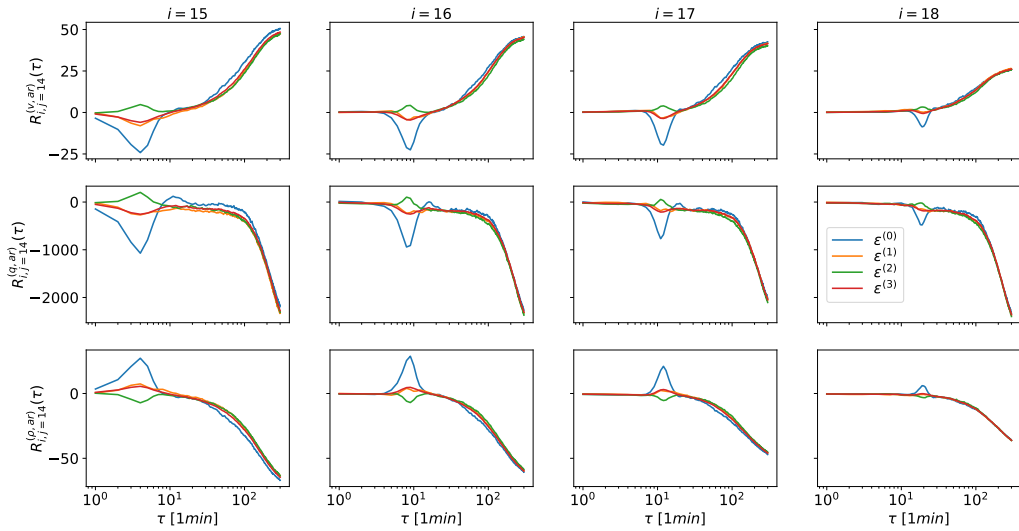
Taking a closer look at the responses for the remaining congestion indicator, one also finds the above described correlations satisfied for all three observables with indicator $\varepsilon^{(2)}(t)$ being a special case. Before discussing the latter, we begin with the more generous velocity range of indicator $\varepsilon^{(3)}(t)$, which demonstrates the importance of choosing smaller velocity ranges to indicate congestion when studying traffic dynamics with response functions. While the minima and maxima of responses to $\varepsilon^{(3)}(t)$ are visible in case of interchange Breitscheid and motorway A3 in Fig. 4(a) and (c), the response at interchange Herne does not exhibit any clear maxima or minima in Fig. 4(b). Thus, it would not be possible to obtain any information about the traffic situation at interchange Herne. In addition, the amplitudes of the local minima and maxima of the responses to $\varepsilon^{(3)}(t)$ show either much smaller values, or values in range of indicator $\varepsilon^{(2)}(t)$ in case of motorway A3 and interchange Breitscheid. Both findings demonstrate that one is able to extract more detailed information about the system by applying multiple indicators. If we restrict a comparison of the remaining three indicators to the case of interchange Breitscheid, we find the amplitudes of the minima (maxima) shrinking (increasing) with increasing values of the velocity ranges. In terms of traffic theory one may expect to find this behavior. During formation of a dense congested phase, i.e. small distances between vehicles moving with small average velocity (e.g. $v < 20$ km/h), an abrupt deceleration to small velocities induces a strong drop of flow rate and increase of local density, respectively. In contrast, less dense congestion



(a) Breitscheid



(b) Herne



(c) Motorway A3

Figure 4: Velocity, flow and density response of spatially subsequent sections i to congestion at (a) section $j = 1$ at interchange Breitscheid during afternoon rush hours, (b) section $j = 11$ at interchange Herne during morning rush hours and (c) section $j = 14$ on motorway A3 during afternoon rush hours.

allows vehicles to move with higher velocities, resulting in smaller drops of flow rate and the decrease of local density. Under the assumption of vehicle count preservation, the hydrodynamic relation in Eq. (1) incorporates this.

The response to indicator $\varepsilon^{(2)}(t)$ shows a behavior opposite to the one of other responses at smaller τ in case of interchange Herne and motorway A3, see Fig. 4(b) and (c). Instead of finding local minima for velocity and flow response, and local maxima for density response, respectively, the responses to indicator $\varepsilon^{(2)}(t)$ exhibit local maxima in case of velocity and flow, and local minima in case of density. This opposite behavior is a result of positive increments $\Delta x_i(t, \tau)$ in Eq. (5) and represents vehicles accelerating during the congestion phase, increasing the flow and lowering the local density. Consequently, the correlations between the three observables remain, but here they express themselves in the opposite case. However, the results depicted in Fig. 4 indicate a difference between the phases of congestion occurring at interchange Breitscheid and the ones occurring at interchange Herne and on motorway A3. Besides the acceleration phase captured by $\varepsilon^{(2)}(t)$, we find a similar case in the flow response for $\varepsilon^{(0)}(t)$ at interchange Breitscheid in Fig. 4(c). A few minutes after the minimum, the response to $\varepsilon^{(0)}(t)$ transitions into a local maximum indicating vehicle acceleration out of the congested traffic. Unfortunately, this only manifests in the flow response and not in velocity or density responses to $\varepsilon^{(0)}(t)$. Although no distinct local maxima occur, there is an increasing course in both responses. Overall, response functions are capable of capturing acceleration phases during congestion, which is an important finding. It can be considered as another foundation for their capability as a tool to study traffic dynamics, especially due to the fact that one is able to identify differences in congestion phases. In addition, it further demonstrates the importance of choosing several indicators in terms of velocity ranges.

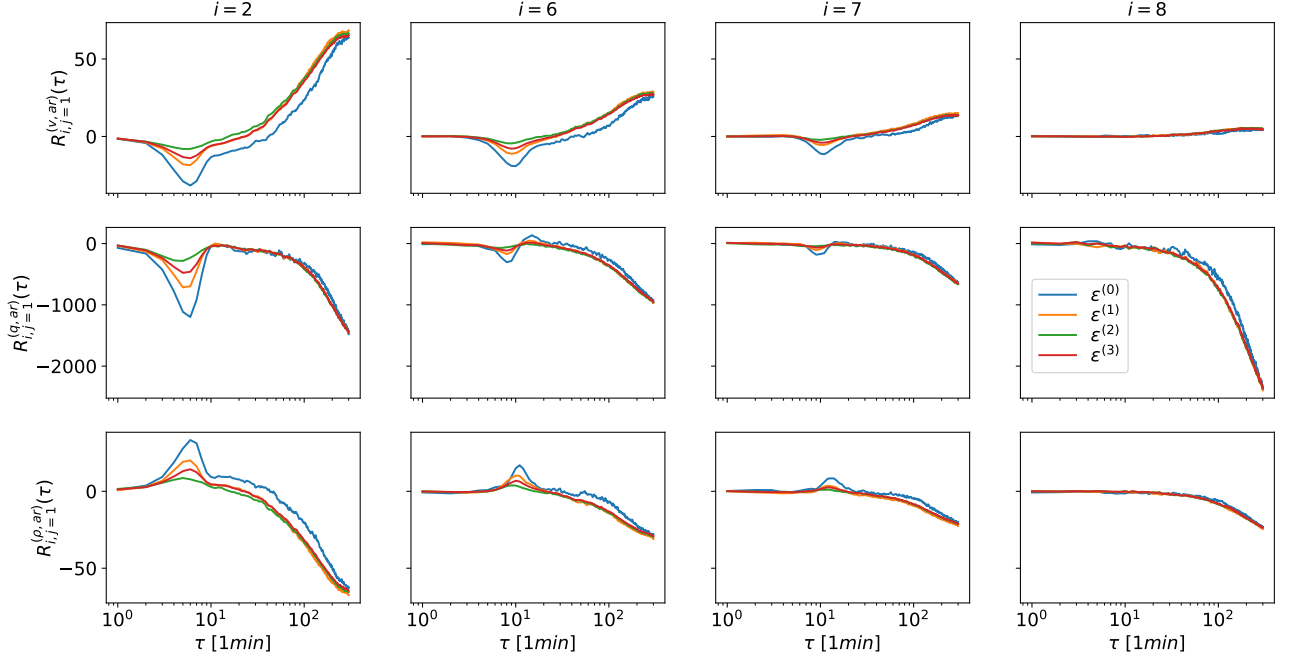
4.2 On- and off-ramp propagation of congestion and generic response features

Besides the results of Sec. 4.1 we are interested in the capability of response functions to detect the propagation of congestion through on- and off-ramps into other parts of the motorway network. Therefore we take a look at two cases at interchange Breitscheid and Herne. In both cases we calculate the responses of spatially subsequent sections along an on-ramp or off-ramp, respectively, to an indicator section on a congested motorway. For interchange Breitscheid we chose section 1 as the indicator section and sections 2 and 6-8 as responding sections, where section 7 is located on the on-ramp leading traffic from motorway A3 onto motorway A52 and section 8 located on motorway A3 (see Fig. 2(a)). In case of interchange Herne we select section 9 as the indicator section and sections 10, 12 and 13 as responding sections, where section 12 is located on the on-ramp leading traffic from motorway A43 onto A42 (see Fig. 2(b)). Figure 5 contains the resulting responses for both cases.

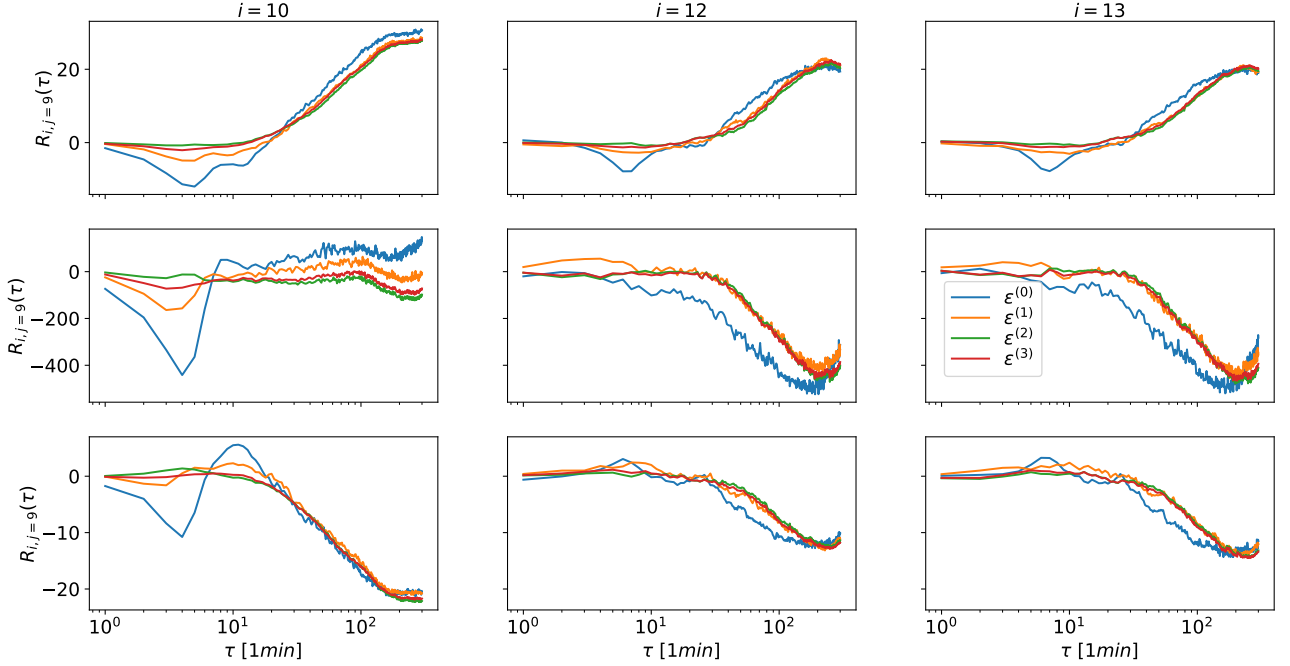
As expected, one initially finds identical responses of all types for section 2 at interchange Breitscheid in Fig. 5(a) (compared with Fig. 4(a)). Furthermore one can identify the propagation of congestion through the on- or off-ramp, respectively, considering the responses of all three traffic variables at sections 6 and 7 to all indicators. Here, the indicating minima (maxima) for $\varepsilon^{(0)}(t)$ are the most distinct. The responses for section 8 do not show any local minima or maxima, implying the congestion does not propagate to section 8. It is worth mentioning that there is no available detector between sections 7 and 8.

In case of interchange Herne one finds a clear indication of congestion propagating through the on- or off-ramp at section 12 regarding the velocity responses to indicator $\varepsilon^{(0)}(t)$ in Fig. 5(b). The comparison between the latter and the corresponding flow responses reveals the incapability of the flow data to identify the congestion propagation in this case. While the flow responses of sections 12 and 13 exhibit a very fluctuating course without any clear local extrema, the responses of section 10 exhibit local minima (and maxima in case of indicator $\varepsilon^{(2)}(t)$). Considering the corresponding density responses one finds an anomaly. The courses of the density responses of sections 12 and 13 to indicator $\varepsilon^{(0)}(t)$ exhibit local maxima fitting the courses of the corresponding velocity responses and therefore the propagation of congestion. In contrast to this, the density response at section 10 exhibits a local minimum instead of an expected local maximum.

Regardless of the possibility to clearly identify congestion propagation through on- or off-ramps in both cases in Fig. 5, we find the unexpected result of the density response for section 10 at interchange



(a) Breitscheid



(b) Herne

Figure 5: Velocity, flow and density response of spatially subsequent sections i to congestion at (a) section $j = 1$ at interchange Breitscheid during afternoon rush hours and (b) section $j = 9$ at interchange Herne during morning rush hours.

Herne. Without any obvious reason from a traffic point of view, or systematic errors, the unexpected result may originate from missing values in the analyzed data. For the indicator section 9 about 14% of that data are missing. For section 10 only 4% of the flow data and 9% of the velocity data is missing. The very fluctuating courses of the flow responses also suggest the potential influence of a low data quality on the anomalous results. Unfortunately, we can not corroborate this point due to a lack of other available data, e.g. on construction sites.

Apart from the congestion propagation, the responses in Fig. 5 and Fig. 4 show similar courses for large time lags τ . Comparing all studied cases one finds velocity responses increasing while flow and density responses decrease with growing time lag τ . Our results imply that this behavior is a generic feature for the individual response types induced by the indicators defined in Eq. (6). These generic courses can be explained by the usual traffic situation represented by the averaged data in Fig. 3. With the increase of time the traffic situation during the rush hours calms down gradually, i.e. the number of traffic participants decreases. As a consequence, a decrease of density and flow enables higher velocities for the remaining traffic participants until the end of rush hours. The generic feature we find is suitable for all responses in our study.

4.3 Differences in congestion patterns

In Sec. 4.1 we find deviant behavior of responses to indicator $\varepsilon^{(2)}(t)$ compared to the other indicators. The deviant behavior clearly indicates an acceleration phase of the vehicles to moderate velocities for sections at interchange Herne in Fig. 4(b) and motorway A3 in Fig. 4(c), but not in case of interchange Breitscheid in Fig. 4(a). The consideration of these results raises the question why this is the case. From a traffic point of view, the results reveal the presence of different congestion patterns. In case of motorway A3 or interchange Herne vehicles are able to accelerate to higher velocities in range of indicator $\varepsilon^{(2)}(t)$ before decelerating again due to the present congestion. As a consequence larger gaps between the traffic participants have to be given, or else vehicles would not be able to accelerate into a higher velocity range. Therefore, the extrema of indicators $\varepsilon^{(0)}(t)$ and $\varepsilon^{(2)}(t)$ that occur at the same time shifts reveal a stop-and-go nature of the congestion pattern at these locations, i.e. acceleration-deceleration cycles. In contrast, the responses for indicators $\varepsilon^{(1)}(t)$ and $\varepsilon^{(2)}(t)$ at interchange Breitscheid do not show any sign of an acceleration phase, i.e. occurring local maxima, during the crucial time period of congestion. This fact indicates a far more dense or synchronized nature in terms of congestion pattern, i.e. vehicles moving with low velocities (in range of $\varepsilon^{(0)}(t)$ and $\varepsilon^{(1)}(t)$) while maintaining small distances to vehicles driving ahead. This does not necessarily exclude a stop-and-go pattern of congestion, but the effect is not strong enough to be captured by the responses.

Due to the nature of the data at hand, it is not possible to verify the above assumptions with information about the distances between traffic participants, therefore we consider the raw data itself. Figure 6 shows a sample of the daily data according to Eq. (4) for all studied locations. In all cases the time period of traffic breakdown can clearly be recognized by considering the course of velocity and density. Due to its very fluctuating nature, the impact on traffic flow is not as clearly visible as in the case of the other observables. The velocity data (first column in Fig. 6) reveals what the averaged responses already indicated. While the velocity at section 3 at interchange Breitscheid almost invariably lies below the range of indicator $\varepsilon^{(2)}(t)$, the velocities at sections 12 and 15 at interchange Herne and on motorway A3, respectively, reach (and exceed) the range of indicator $\varepsilon^{(2)}(t)$ frequently. Even though a traffic oscillation, i.e. a stop-and-go pattern, is clearly recognizable in the velocities at all three locations, the corresponding responses in Fig. 4 only show an acceleration phase, i.e. local maxima, for indicator $\varepsilon^{(2)}(t)$ in case of interchange Herne and motorway A3. Considering the velocity at section 3 at Breitscheid in Fig. 6 one may expect to see a local maximum in the response to indicator $\varepsilon^{(1)}(t)$, due to the fact that the velocity exceeds the range of indicator $\varepsilon^{(0)}(t)$ frequently, but this is not the case.

One possible explanation for the absence of a visible acceleration phase in the response to indicator $\varepsilon^{(1)}(t)$ at Breitscheid is the frequency at which the sample velocity distribution occurs, i.e. the latter is a rare case on average and the velocity does not exceed the range of indicator $\varepsilon^{(1)}(t)$ as often as in the sample in Fig. 6(a). Due to the fact that the response functions detect an average change,

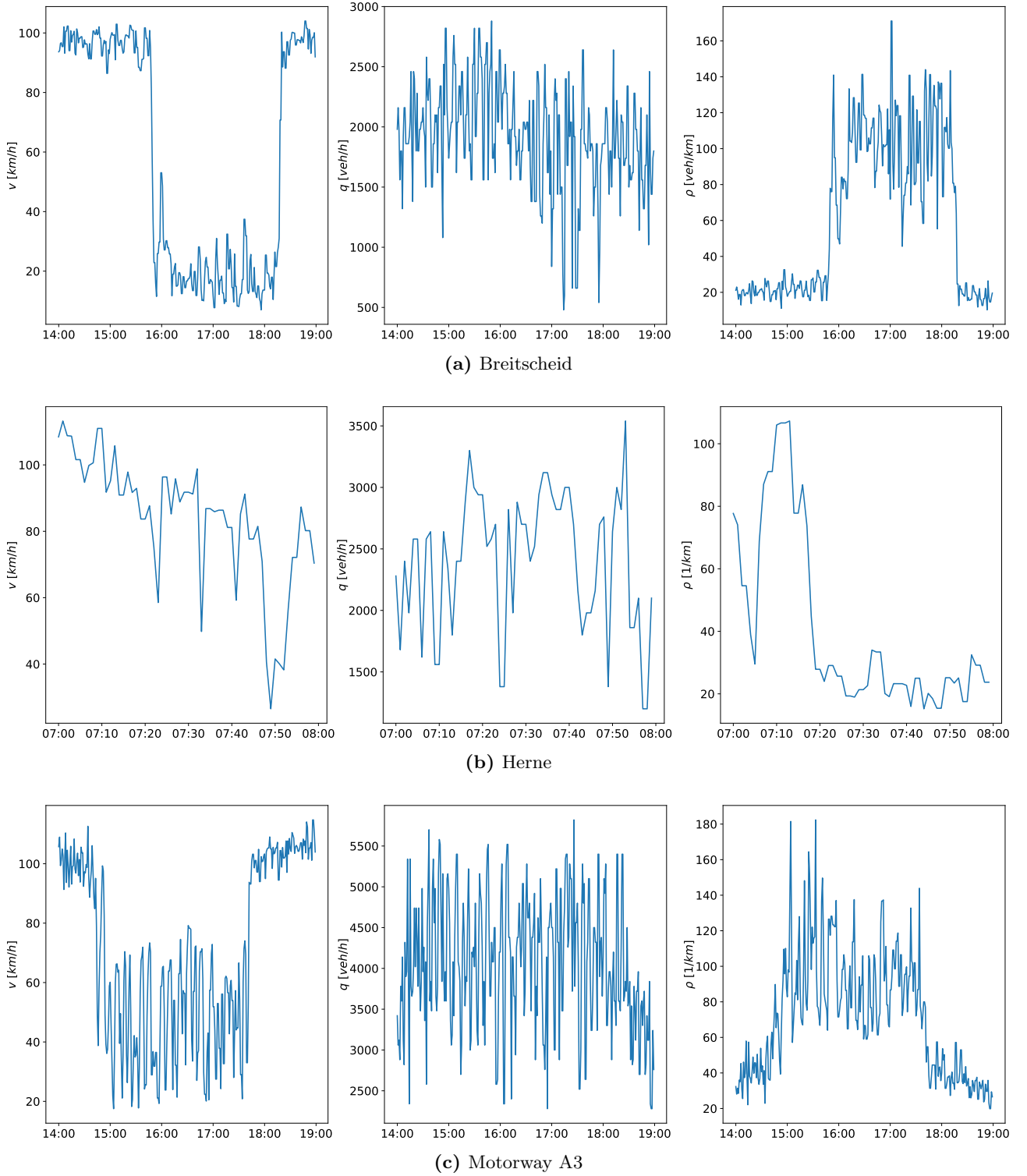


Figure 6: Sample of the daily data for (a) section 3 at interchange Breitscheid during afternoon rush hours, (b) section 12 at interchange Herne during morning rush hours and (c) section 15 on motorway A3 during afternoon rush hours. The data in (a) and (c) were recorded on Tuesday, December 13, 2016, the data in (b) on Wednesday, April 26, 2017.

another possible explanation would be a difference in frequency of the traffic oscillation itself. Therefore, we take a closer look at the data sample in Fig. 7. Counting the number of traffic oscillations, i.e. the transition from one velocity minimum into the next velocity minimum (which is around 10 km/h for Breitscheid and around 25 km/h for A3 in Fig. 7), during the first 30 minutes of the rush hours one finds five oscillations in case of motorway A3 and three oscillations in case of interchange Breitscheid. Based on the sample, this would imply that the temporal frequency of the traffic oscillation on motorway A3 is almost twice as high as the one at interchange Breitscheid.

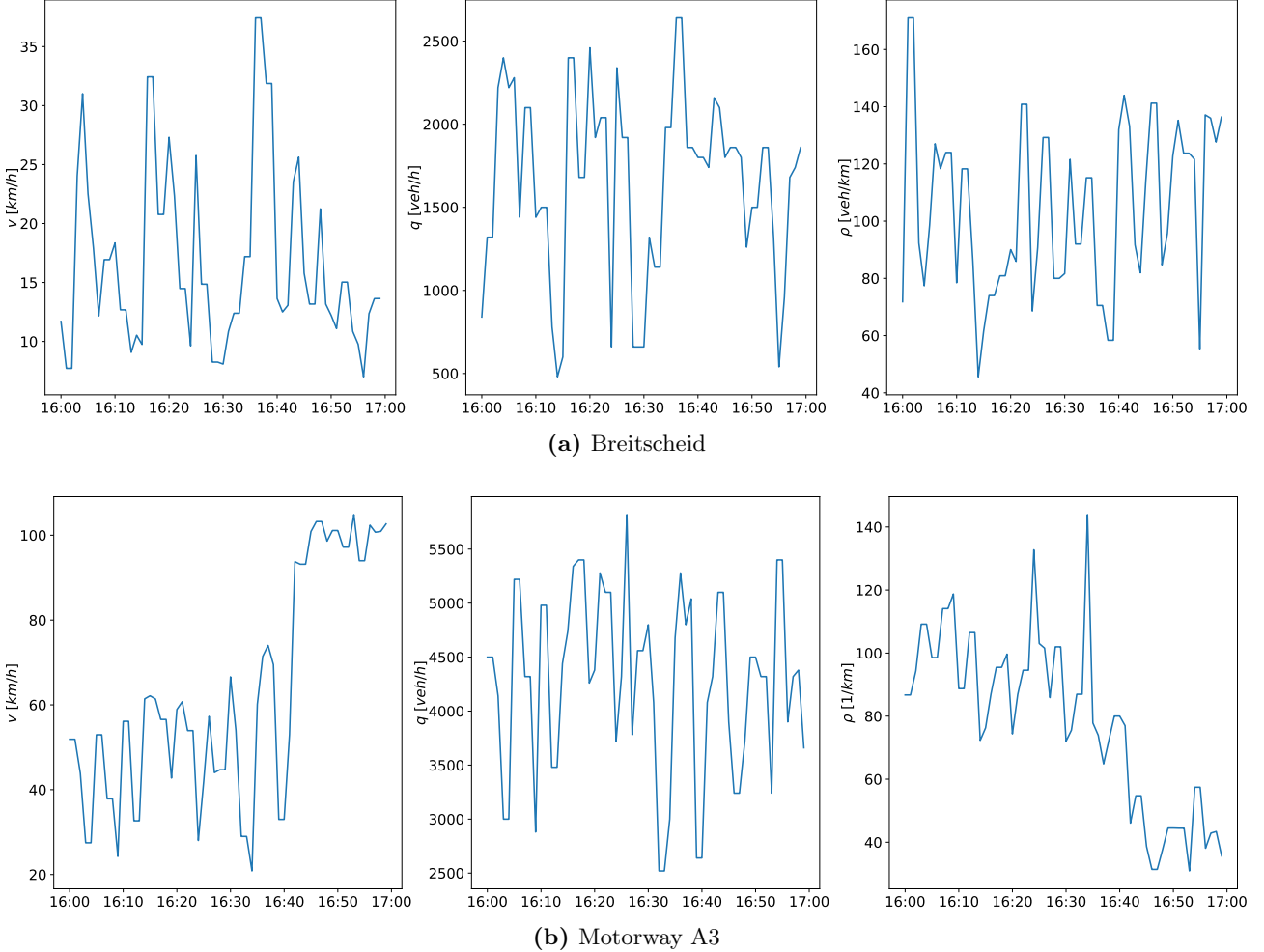


Figure 7: Zoom into the time period from 16:00 to 17:00 of the daily data from Fig. 6 for (a) section 3 at interchange Breitscheid and (b) section 15 on motorway A3.

Apart from the above statements, which could already be derived from the response functions, one may be able to establish a connection between the width of the valleys in the course of the responses and the periodicity of the traffic oscillation. Since the valleys (hills) represent a sequence of deceleration and acceleration (acceleration and deceleration) one may expect their width (regarding the τ -axis) to coincide with the average time it takes to traverse such a sequence during congestion. To test this assumption we again consider the data sample in Fig. 7 and compare the period length of the traffic oscillation with the width of the valleys in the course of the responses. Therefore, we take into account the range of velocities depicted in the samples. For interchange Breitscheid we find a period of roughly 10 minutes for the traffic oscillation with occurring velocities between 5 km/h and 35 km/h in Fig. 7(a). Comparing this with the corresponding indicators $\varepsilon^{(0)}(t)$ and $\varepsilon^{(1)}(t)$ in Fig. 4(a) we find the width of the valleys is also roughly 10 minutes and therefore in accordance with the period. With the exception of the density response, whose signal curve is blurred, the coincidence is also found for the flow. In case of motorway A3 the sample in Fig. 7(b) mostly shows velocities between 25 km/h and 60 km/h and an oscillation period about 5 minutes. A comparison of the latter with the width of the valleys in the responses to indicators $\varepsilon^{(1)}(t)$ and $\varepsilon^{(2)}(t)$ in Fig. 4(c) also shows the coincidence in

case of velocity, flow and density. These findings corroborate the above results regarding the temporal frequency of the traffic oscillations.

Lastly, we would like to make a brief remark on the classification of the found congestion patterns according to three-phase traffic theory. A full analysis on the identification of traffic phases or phase transitions is out of the scope of this study, but it is worth showing a small glimpse of the potential that response functions offer for this purpose. The above findings suggest that the congestion at interchange Breitscheid and on motorway A3 are very likely to be wide moving jams. This conclusion can be traced back to two fundamental properties of wide moving jams [14]. On the one hand a wide moving jam propagates upstream through any traffic state and bottleneck with a constant mean velocity of its downstream jam front. On the other hand wide moving jams have a significant spatial (longitudinal) expansion. In case of interchange Breitscheid the responses indicate congestion with a spatial expansion of about 4.2 km (distance between sections 1 and 5) which propagates through a bottleneck at section 6 (see Sec. 4.2 and Fig. A1 in Appendix A.1). The responses to sections on motorway A3 indicate that congestion propagates an even longer distance, here the spatial extension is about 8.8 km (distance between sections 14 and 19). These findings can be derived from the calculated responses without taking into account any additional data and deliver strong evidence for the classification of the congestion as a wide moving jam.

4.4 The propagation velocity of congestion

We aim to derive the propagation velocity of congestion from the responses to further strengthen the conclusions from Sec. 4.3. Figure 8 depicts the velocity responses for sections on motorway A3 already shown in Fig. 4(c) broken down by the individual indicators. This representation emphasizes the propagation nature of the minima and maxima, and therefore the propagation of congestion, in a very clear fashion. This clearly striking representation by itself gives rise to the question if it is possible to derive the propagation velocity v_c of congestion from our results, which values typically lie between 15 km/h and 20 km/h [14,27]. To answer the question we determine the propagation velocity of congestion from all types of responses for interchange Breitscheid and motorway A3. A complete overview of all responses for both locations in the representation of Fig. 8 is given in Fig. A2 in the Appendix A.2. To determine the propagation velocities, we work out the positions of the corresponding local minima (or maxima) in the response curves for two sections k and l to retrieve the time lag difference $\Delta\tau_{kl}^{(\sigma)}$. Dividing the distance $d_{kl}^{(x)}$ between the two sections by the corresponding time lag difference determines the propagation velocity $v_{\text{prop}}^{(x)}$ of the congestion:

$$v_{\text{prop}}^{(x)} = \frac{d_{kl}}{\Delta\tau_{kl}^{(\sigma,x)}}, \quad (7)$$

where $x = v, q, \rho$ denotes the type of response and $\sigma = \text{min, max}$ the type of local extremum that has to be taken into account.

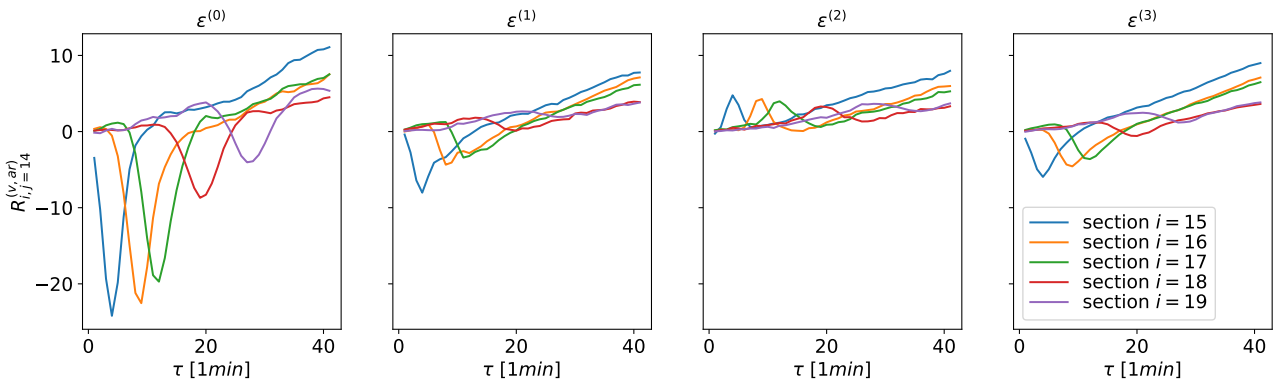


Figure 8: Velocity response of spatially subsequent sections i to congestion at section $j = 14$ on motorway A3 during afternoon rush hours broken down by the individual indicators $\varepsilon(t)$.

Figure 9 shows the propagation velocities for both considered cases. Regarding the result of interchange Breitscheid we point out that section 6 is a special case due to its location (see Secs. 3 and 4.2, and Fig. A1 in Appendix A.1), and therefore separated with a dashed line in Fig. 9 (a). In general, we find the values of the propagation velocities either very close to or within the typical interval of v_c . In the majority of cases the values of v_{prop} decrease into the numerical range of v_c with increasing distance to the indicator section j . In other cases, the values of v_{prop} derive from this behavior by scattering, e.g. $v_{\text{prop}}^{(\rho)}$ for Breitscheid in Fig. 9(a) (last row) as well as $v_{\text{prop}}^{(q)}$ for motorway A3 in Fig. 9(b) (second row). A comparison of these cases with the corresponding responses in Fig. 4 (or Fig. A2) shows that the scattering can be ascribed to the quality of the responses. The shape of the valleys and position of the extrema are not as clearly manifested as in other cases, therefore it is difficult to accurately calculate the related propagation velocities. Nevertheless, the numerical values lie within the typical range of v_c . Unfortunately, it is not possible to derive a generic behavior on the basis of the results in Fig. 9 due to the scattering of values.

In view of the fact that we derive the propagation velocities from the averaged response functions in an initial approach, we consider the results to be satisfying. Even though the velocities were determined for all indicators separately, the results are close to each other. The results are not conclusive enough to derive a generic behavior regarding the dependence of the distance to the indicator section j . However, it is not our goal to carry out a complete analysis within the scope of this contribution, but the above results demonstrate a proof of concept. In case of the classification of the congestion as wide moving jams, the results do not argue against it.

4.5 Scaling of responses

The similarities in shape of the responses for smaller time shifts τ are conspicuous and lead to the question of scalability. Here we try to identify a possible scaling behavior by applying the following approach. Let μ_i be the peak position of the i -th response curve and σ_i the corresponding full width half maximum. We define

$$\tau_s^{(i)} = \frac{\tau - \mu_i}{\sigma_i} \quad (8)$$

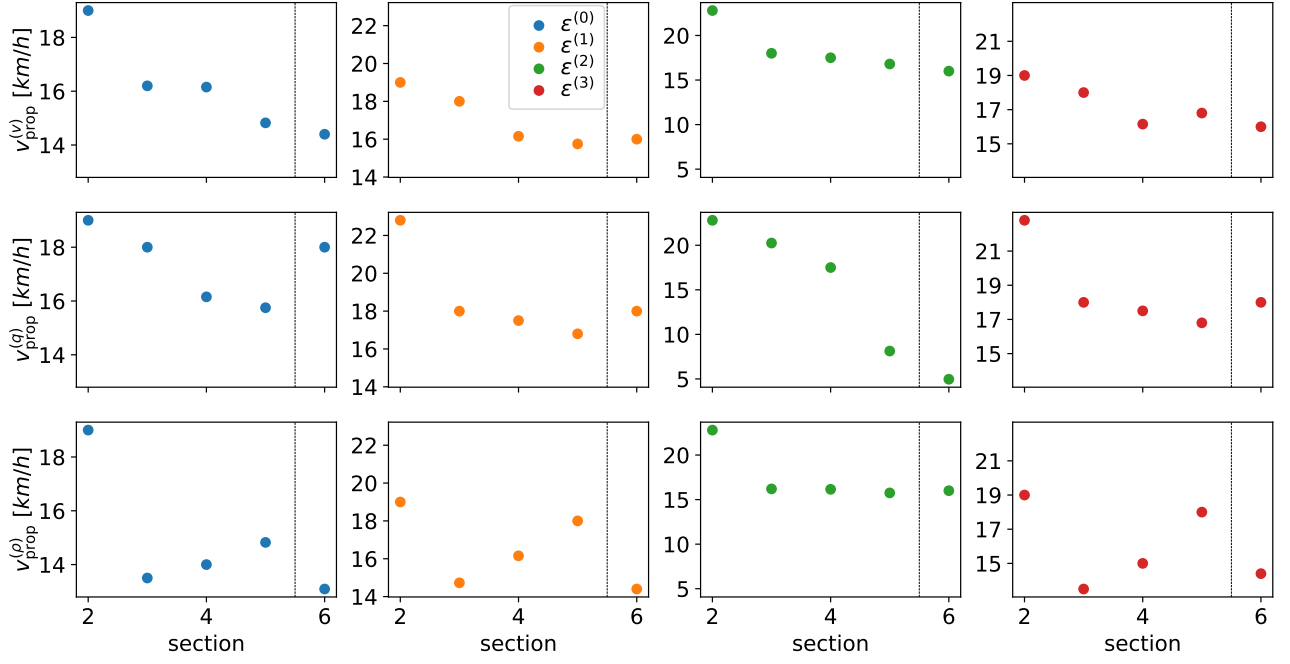
as a rescaled axis for the time shift τ . In addition, we scale the responses with a factor $\alpha_i = 1/\sigma_i$ resulting in the scaling function

$$S_i(\tau_s) = \frac{1}{\sigma_i} R_i(\tau_s^{(i)}). \quad (9)$$

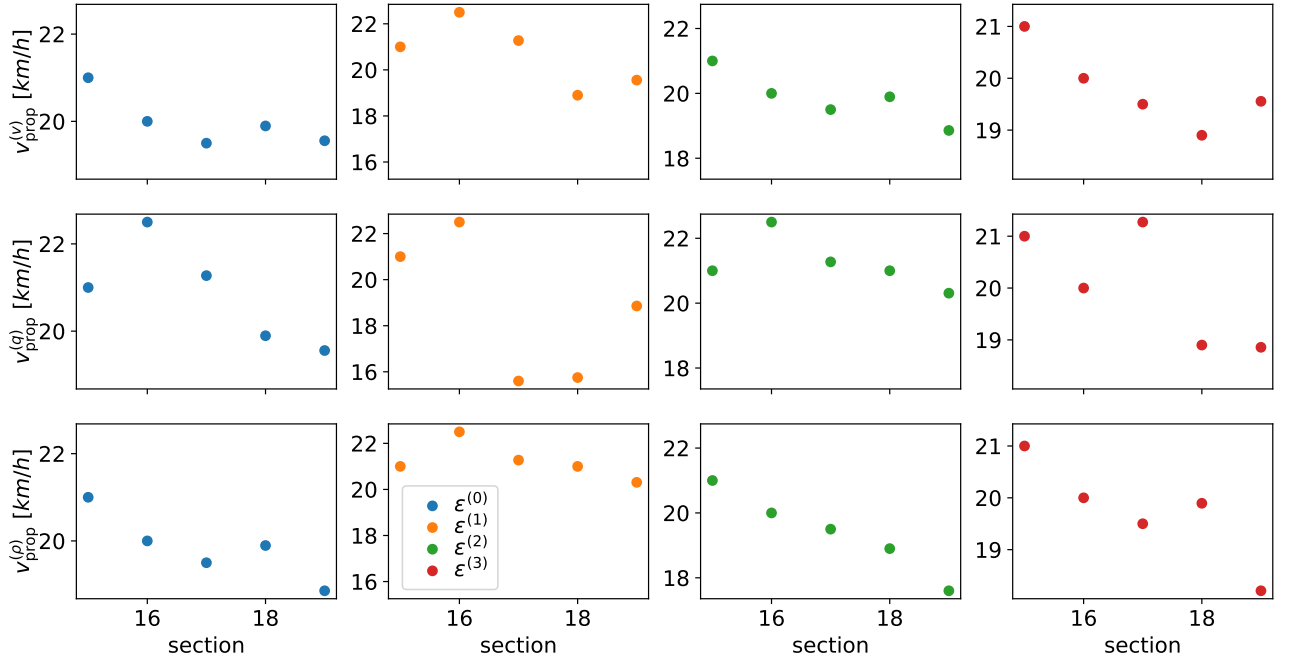
Figure 10 shows examples of velocity responses and their respective rescaling according to Eq. (9) in case of Breitscheid and motorway A3. For the depicted cases the chosen scaling method works well. However, the success of the applied scaling method highly depends on the manifestation of the peaks, or valleys, respectively. In some cases it is not possible to scale our results properly. The determination of the full width half maximum σ_i is difficult if peaks, or valleys, in the course of responses are not clearly shaped. Nevertheless, the examples depicted in Fig. 10 successfully demonstrate a proof of concept. It is not our goal to carry out a complete analysis of scaling methods and behavior within the scope of this contribution, but the results of our demonstration are satisfying.

5 Conclusion

Response functions of the fundamental traffic observables velocity, flow and density were analyzed based on congestion indicators for different velocity ranges and spatial subsequent sections on heavily trafficked motorways in NRW, Germany. All three response types of observables clearly showed valleys (hills), or local minima (maxima) within the first 30 minutes of time lags, capturing the impact of congestion and its propagation over several kilometers. We found the correlation between the three fundamental observables reproduced by the responses and showed the importance of considering multiple indicators with different velocity ranges to indicate congestion. We also verified congestion propagating through on- and off-ramps of interchanges into other parts of the motorway network.



(a) Breitscheid



(b) Motorway A3

Figure 9: Propagation velocities v_{prop} resulting from the minimal and maximal strength of the responses of each observable to each indicator at (a) interchange Breitscheid and (b) motorway A3. The original responses are depicted in Fig. A2. The dashed line in (a) visually separates section 6 from the other sections due to its location.

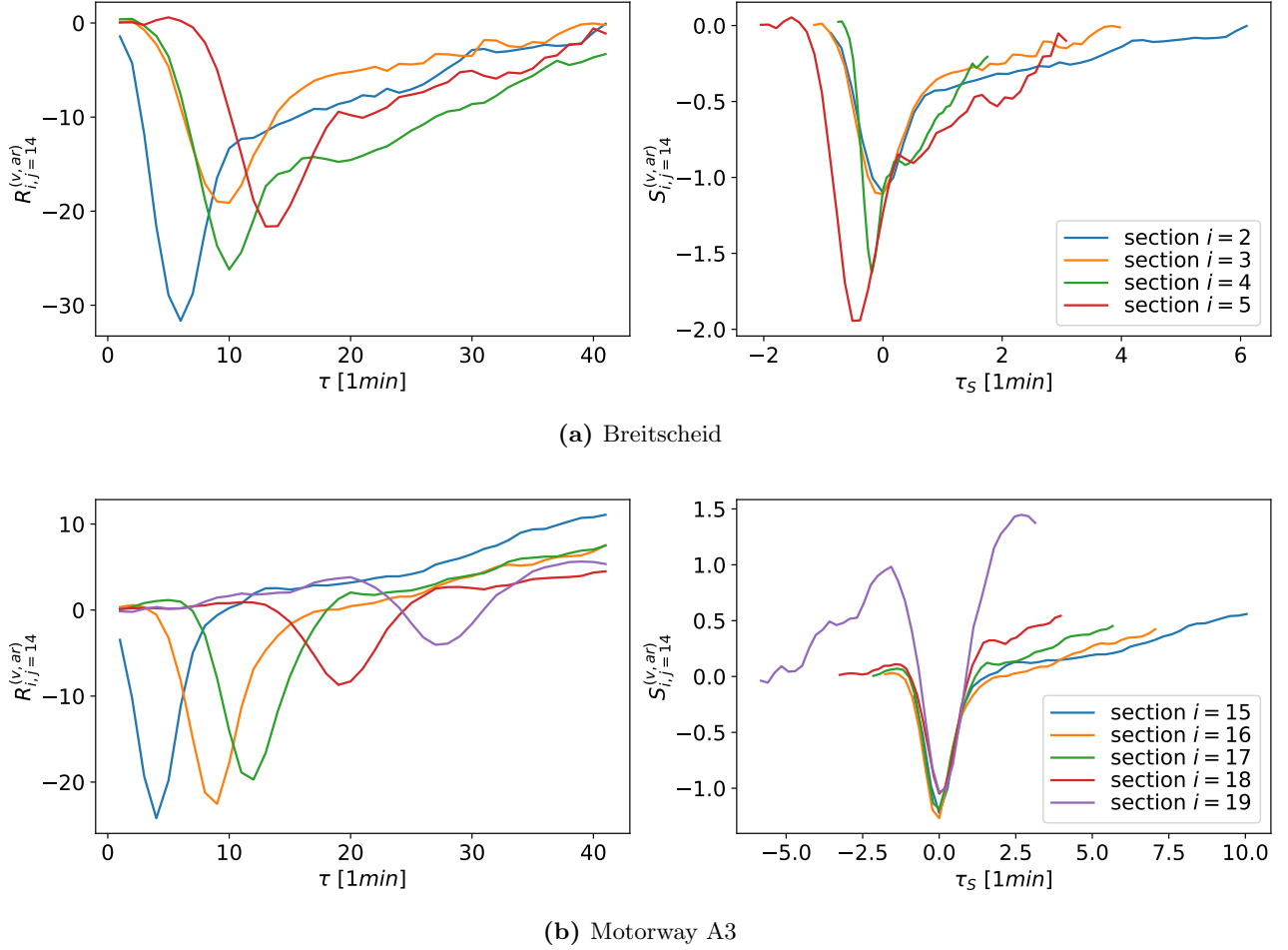


Figure 10: Original (left column) and rescaled (right column) velocity responses of spatially subsequent sections i to congestion at (a) section $j = 1$ at Breitscheid and (b) section $j = 14$ on motorway A3 during afternoon rush hours for indicator $\varepsilon^{(0)}(t)$.

Furthermore, via responses, we captured the acceleration-deceleration cycles of traffic participants during congestion, which reflect traffic oscillations, i.e. stop-and-go patterns. Based on this finding we further differentiated congestion patterns with the help of response functions. By considering a sample of the given data we found that the width of the valleys (hills) in the course of the responses coincides with the average period of the occurring traffic oscillations. In addition, we narrowed down congestion phases according to three-phase traffic theory with information gathered from the responses. Motivated by the latter, we derived the propagation velocity of congestion from the responses. Even though the numerical results agree well with empirical observations, it was not possible to derive a generic relation between the propagation velocities and the distance to the indicator section. Lastly, motivated by the similarities in shape of the responses for small time shifts, we successfully conducted an approach for demonstrating scaling behavior of the responses.

The findings of our contribution demonstrate the potential for using response functions as a tool to study traffic dynamics and analyze occurring traffic patterns. Responses reveal the change of traffic observables at given road sections based on prior congestion at other sections. Information of this kind is very useful in applications of traffic engineering, e.g. for estimating, tracking or predicting traffic patterns. A major advantage of the response approach is that it avoids complex calculations and parameter predictions required for the application of various models. Moreover, the presented approach can be conducted with a higher level of details. It is very likely that a more accurate analysis of traffic patterns can be made by determining the responses for each individual lane. The latter is of particular interest with regard to the formation of congestion patterns, their characterization and the determination of their propagation velocity. Possible follow-up studies in this direction seem to be very promising to uncovering further potential of response functions as a useful tool for traffic scientists and engineers.

Acknowledgements

We gratefully acknowledge the support from Deutsche Forschungsgemeinschaft (DFG) within the project “Korrelationen und deren Dynamik in Autobahnnetzen” (No. 418382724). We also thank Straßen.NRW for providing the empirical traffic data.

Author contributions

M.S. and T.G. proposed the research. S.G. prepared the traffic data, performed all calculations, and wrote the manuscript with input from S.W., T.G. and M.S. All authors contributed equally to analyzing the results and reviewing the paper.

References

- [1] M.J. Lighthill, G.B. Whitham. On Kinematic Waves. II. A Theory of Traffic Flow on Long Crowded Roads. *Proc. R. Soc.*, A229, 317-345, 1955. doi: 10.1098/rspa.1955.0089
- [2] G. F. Newell, Mathematical Models for Freely-Flowing Highway Traffic. *Operations Res.*, 3(2): 176-186, 1955. doi: 10.1287/opre.3.2.176
- [3] P.I. Richards. Shock Waves on the Highway. *Operations Res.* 4(1): 42-51, 1956. doi: 10.1287/opre.4.1.42
- [4] E. Kometani, T. Sasaki, A Safety Index for Traffic with Linear Spacing. *Operations Res.*, 7(6): 704-720, 1959. doi: 10.1287/opre.7.6.704
- [5] D. C. Gazis, R. Herman and R. W. Rothery. Nonlinear Follow-the-Leader Models of Traffic Flow. *Operations Res.*, 9(4): 545-567, 1961. doi: 10.1287/opre.9.4.545
- [6] H.J. Payne, FREFLO: A macroscopic simulation models of freeway traffic. *TRR*, 772, 68–75, 1979.

- [7] P.G. Gipps, A behavioural car-following model for computer simulation. *Trans. Res. B*, 15(2): 105-111, 1981. doi: 10.1016/0191-2615(81)90037-0
- [8] K. Nagel and M. Schreckenberg. A cellular automaton model for freeway traffic. *J. Phys. I*, 2:2221, 1992. doi:10.1051/jp1:1992277.
- [9] A. Schadschneider and M. Schreckenberg. Cellular automation models and traffic flow. *J. Phys. A: Math. Gen.*, 26(15):L679-L683, 1993. doi: 10.1088/0305-4470/26/15/011.
- [10] M. Schreckenberg, A. Schadschneider, K. Nagel, and N. Ito. Discrete stochastic models for traffic flow. *Phys. Rev. E*, 51:2939-2949, 1995. doi: 10.1103/PhysRevE.51.2939.
- [11] R. Barlovic, L. Santen, A. Schadschneider, and M. Schreckenberg. Metastable states in cellular automata for traffic flow. *Eur. Phys. J. B*, 5(3):793-800, 1998. doi: 10.1007/s100510050504.
- [12] G. F. Newell, A simplified car-following theory: a lower order model. *Trans. Res. B*, 36(3): 195-205, 2002. doi: 10.1016/S0191-2615(00)00044-8
- [13] B. S. Kerner, S. L. Klenov, D. E. Wolf. Cellular automata approach to three-phase traffic theory. *J. Phys. A: Math. Gen.*, 35(47): 9971–10013, 2002. doi: 10.1088/0305-4470/35/47/303
- [14] B. S. Kerner. *The Physics of Traffic: Empirical Freeway Pattern Features, Engineering Applications, and Theory*. Springer, 2004. doi: 10.1007/978-3-540-40986-1.
- [15] B. S. Kerner. *Introduction to Modern Traffic Flow Theory and Control: The Long Road to Three-Phase Traffic Theory*. Springer, 2009. doi: 10.1007/978-3-642-02605-8.
- [16] S. Wang, S. Gartzke, M. Schreckenberg, and T. Guhr. Quasi-stationary states in temporal correlations for traffic systems: Cologne orbital motorway as an example. *J. Stat. Mech. Theory Exp.*, 2020:103404, 2020. doi: 10.1088/1742-5468/abbcd3.
- [17] S. Wang, S. Gartzke, M. Schreckenberg, and T. Guhr. Collective behavior in the North Rhine-Westphalia motorway network. *J. Stat. Mech. Theor. Exp.*, 2021:123401, 2021. doi: 10.1088/1742-5468/ac3662
- [18] S. Gartzke, S. Wang, T. Guhr, and M. Schreckenberg. Spatial correlation analysis of traffic flow on parallel motorways in Germany. *Physica A*, 599:127367, 2022. doi: 10.1016/j.physa.2022.127367
- [19] S. Wang, M. Schreckenberg, and T. Guhr. Identifying subdominant collective effects in a large motorway network. *J. Stat. Mech.* 2022:113402, 2022. doi: 10.1088/1742-5468/ac99d4
- [20] S. Wang, M. Schreckenberg and T. Guhr. Response functions as a new concept to study local dynamics in traffic networks. *Phys. A: Stat. Mech. Appl.*, Vol. 626, 129116, 2023. doi: 10.1016/j.physa.2023.129116.
- [21] J.-P. Bouchaud, Y. Gefen, M. Potters, and M. Wyart. Fluctuations and response in financial markets: the subtle nature of 'random' price changes. *Quant. Finance*, 4(2):176-190, 2003. doi: 10.1088/1469-7688/4/2/007
- [22] S. Wang, R. Schäfer and T. Guhr. Cross-response in correlated financial markets: individual stocks. *Eur. Phys. J. B*, 89(105):105, 2016. doi: 10.1140/epjb/e2016-60818-y
- [23] S. Wang, R. Schäfer and T. Guhr. Average cross-responses in correlated financial markets. *Eur. Phys. J. B*, 89(207):207, 2016. doi: 10.1140/epjb/e2016-70137-0
- [24] S. Wang and T. Guhr. Microscopic understanding of cross-responses between stocks: a two-component price impact model. *MML*, 3(03n04):1850009, 2017. doi: 10.1142/S2382626618500090
- [25] M. Benzaquen, I. Mastromatteo, Z. Eisler, and J.-P. Bouchaud. Dissecting cross-impact on stock markets: An empirical analysis. *J. Stat. Mech. Theor. Exp.*, 2017(2):023406, 2017. doi: 10.1088/1742-5468/aa53f7

- [26] J. C. Henao-Londono, S. M. Krause and T. Guhr. Price response functions and spread impact in correlated financial markets. *Eur. Phys. J. B*, 94(78):78, 2021. doi: 10.1140/epjb/s10051-021-00077-z
- [27] M. Treiber and A. Kesting. *Verkehrsdynamik und -simulation*. Springer Berlin Heidelberg, Berlin, Heidelberg, 2010. doi:10.1007/978-3-642-05228-6_1.
- [28] Copyright and License for OpenStreetMap. <https://www.openstreetmap.org/copyright>.
- [29] Open Data Commons Open Database License v1.0. <https://opendatacommons.org/licenses/odbl/1-0/>.
- [30] License for Paint.net <https://www.getpaint.net/license.html>

Appendices

Appendix A

A.1 Interchange Breitscheid: supplementary map

Figure A1 shows the details of the map for interchange Breitscheid in Fig. 2(a) to illustrate the special location of section 6 on a separate lane. The latter merges the incoming traffic flows from connected motorways A524 and A3 which is indicated by black arrows. After passing section 6, the traffic flow is merged into the lanes of motorway A52.



Figure A1: Zoom into the map of interchange Breitscheid shown in Fig. 2(a). Section 6 is located on a separated lane, merging traffic flows from connected motorways A524 and A3 indicated by black arrows.

A.2 Different representation of responses

Figure A2 shows the velocity, flow and density responses of sections at interchange Breitscheid and motorway A3 broken down by individual indicators for congestion. It serves as supplemental information of Fig. 4 because it emphasizes the propagating nature of the congestion in a more clear fashion.

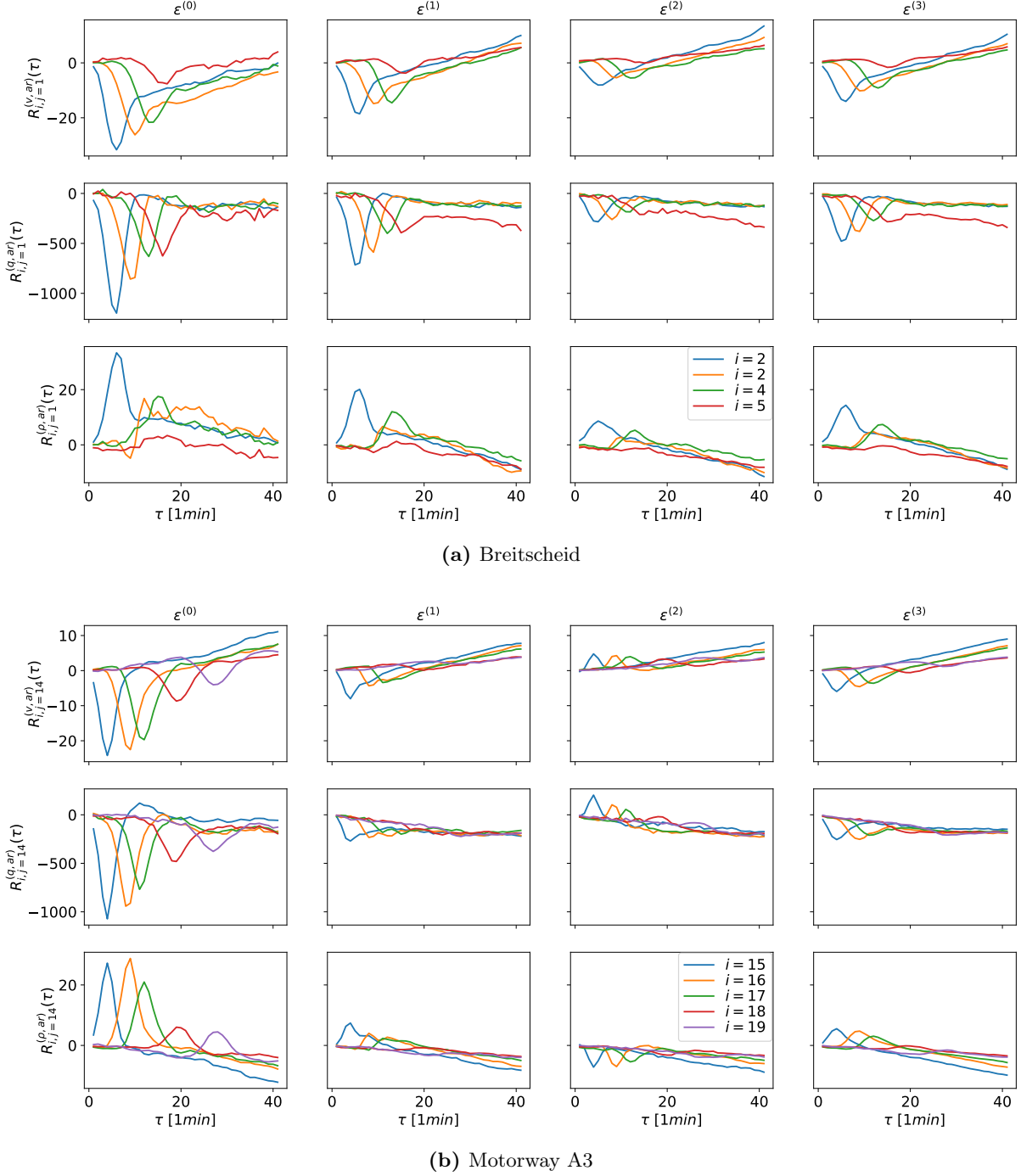


Figure A2: Velocity, flow and density response of spatially subsequent sections i to congestion at (a) section $j = 1$ at interchange Breitscheid during afternoon rush hours and (b) section $j = 14$ on motorway A3 during afternoon rush hours broken down by the individual indicators $\epsilon(t)$.